

Loss of Polycystin-1 in Human Cyst-Lining Epithelia Leads to Ciliary Dysfunction

Surya M. Nauli,* Sandro Rossetti,† Robert J. Kolb,* Francis J. Alenghat,‡
Mark B. Consugar,† Peter C. Harris,† Donald E. Ingber,‡ Mahmoud Loghman-Adham,§ and
Jing Zhou*

*Renal Division, Department of Medicine, Brigham and Women's Hospital and Harvard Medical School, Boston, Massachusetts; †Division of Nephrology, Mayo Clinic College of Medicine, Rochester, Minnesota; ‡Vascular Biology Program, Departments of Pathology and Surgery, Children's Hospital and Harvard Medical School, Boston, Massachusetts; and §Department of Pediatrics and Pediatrics Research Institute, St. Louis University School of Medicine, St. Louis, Missouri

A “two-hit” hypothesis predicts a second somatic hit, in addition to the germline mutation, as a prerequisite to cystogenesis and has been proposed to explain the focal nature for renal cyst formation in autosomal dominant polycystic kidney disease (ADPKD). It was reported previously that *Pkd1*^{null/null} mouse kidney epithelial cells are unresponsive to flow stimulation. This report shows that *Pkd1*^{+/null} cells are capable of responding to mechanical flow stimulation by changing their intracellular calcium concentration in a manner similar to that of wild-type cells. This paper reports that human renal epithelia require a higher level of shear stress to evoke a cytosolic calcium increase than do mouse renal epithelia. Both immortalized and primary cultured renal epithelial cells that originate from normal and nondilated ADPKD human kidney tubules display normal ciliary expression of the polycystins and respond to fluid-flow shear stress with the typical change in cytosolic calcium. In contrast, immortalized and primary cultured cyst-lining epithelial cells from ADPKD patients with mutations in *PKD1* or with abnormal ciliary expression of polycystin-1 or -2 were not responsive to fluid shear stress. These data support a two-hit hypothesis as a mechanism of cystogenesis. This report proposes that calcium response to fluid-flow shear stress can be used as a readout of polycystin function and that loss of mechanosensation in the renal tubular epithelia is a feature of PKD cysts.

J Am Soc Nephrol 17: 1015–1025, 2006. doi: 10.1681/ASN.2005080830

A gene mutation can result in disease through direct or indirect mechanisms. For instance, in the gain-of-function mutation, a germline mutant allele confers new or enhanced protein activity with a pathologic function, whereas a dominant-negative mutation produces an aberrant protein that interferes with the function of the normal protein. In haploinsufficiency, a loss of 50% of normal protein as a result of a mutation in one of its alleles is sufficient to cause disease. In the *two-hit mechanism*, the disease results from a germline mutation in one allele, followed by the subsequent acquisition of a somatic mutation in the second normal allele with no remaining functional protein.

Autosomal dominant polycystic kidney disease (ADPKD) is the most common hereditary kidney disease. *PKD1* and *PKD2* are the genes that encode for the polycystin-1 (PC1) and polycystin-2 (PC2) proteins, respectively. Although patients with ADPKD carry heterozygous mutations in either *PKD1* or *PKD2* and present 100% penetrance of cystic kidney phenotypes, fewer than 5% of nephrons form cysts. These fluid-filled cysts

are lined by a single layer of epithelial cells and can occur at any site along the nephron. The presence of renal cysts in ADPKD, despite the low number, results in a gradual decline in renal function. To explain the focal nature of renal cyst formation in ADPKD, Reeders (1) proposed a “two-hit” hypothesis suggesting that a second somatic alteration to the gene, in addition to a germline mutation, is a prerequisite to the disease phenotype. Although a mechanism based on haploinsufficiency has not been excluded, somatic mutations in either *PKD1* or *PKD2* indeed have been found in several ADPKD cyst-lining epithelia (2–8), even though a somatic loss of other chromosomes or mutations in other loci also are found (2). These data provided hints that ADPKD is a recessive disease at the cellular level. The lack of a cellular assay for PC1 function has prevented an experimental demonstration of loss of function in cyst-lining epithelia in ADPKD.

We and others have shown previously that PC1 and PC2 are localized to the primary cilia (9). The mechanosensation function of polycystins can be assayed in cultured mouse kidney epithelial cells by monitoring changes in the intracellular calcium concentration in response to fluid-flow shear stress (10). To test the loss-of-function hypothesis in ADPKD with regard to mechanosensory ability, we used the flow assay to examine shear stress-induced calcium responses in cells that were derived from a heterozygous *Pkd1* mouse model. Furthermore, we

Received August 8, 2005. Accepted February 1, 2006.

Published online ahead of print. Publication date available at www.jasn.org.

Address correspondence to: Dr. Jing Zhou, Harvard Institutes of Medicine, Suite 520, 77 Avenue Louis Pasteur, Boston, MA 02115. Phone: 617-525-5860; Fax: 617-525-5861; E-mail: zhou@rics.bwh.harvard.edu

characterized the responses in immortalized and primary cultured cells that originated from normal and ADPKD human kidneys. We analyzed cells that were derived from cyst (dilated tubules) and nondilated tubules of the same ADPKD kidneys. Our data support a two-hit, loss-of-function model for ADPKD in which the ciliary mechanosensation of fluid-flow shear stress by polycystins is lost.

Materials and Methods

Cell Culture

Mouse kidney epithelial cells (*Pkd1*^{+/+}, *Pkd1*^{+/null}, and *Pkd1*^{null/null}) were isolated from embryonic day 15.5 kidneys from a cross of *Pkd1*^{+/null} mice that also carry a temperature-sensitive simian virus 40 (SV40) large T-antigen transgene (11,12). Thus, the resulting cell lines were conditionally immortalized, and the expression of the SV40 large T-antigen was regulated by temperature and IFN- γ .

Human cell lines from renal cortical tubular epithelia (RCTE) and ADPKD cyst-lining epithelia (9-12 and 9-7 cell lines) were immortalized with recombinant ori⁻ adeno-SV40 viruses. All cell lines were cloned by positive selection for both epithelial and collecting tubular markers (cytokeratin and *Dolichus biflorus* agglutinin [DBA]) as described previously (10,13).

The primary cultured cells that were used in this study were freshly dissociated and cultured from individual tubules from a single normal kidney or from cysts that were collected from three ADPKD kidneys by a method described previously (13). Cells were grown and differentiated on glass coverslips for all flow and immunolabeling experiments. Unless stated otherwise, all cell culture reagents were purchased from Invitrogen (Carlsbad, CA).

Fluorescence Automated Cell Sorting

Differentiated cells were rinsed with PBS, and approximately 10⁴ viable cells were analyzed for co-expression of epithelial and collecting tubular markers. Cells were incubated with primary antibodies to cytokeratin (1:200) at room temperature for 1 h followed by incubation with the secondary antibody, TX Red (1:500), for another hour. FITC-conjugated DBA (10 μ g/ml) then was applied to the cells at room temperature for 1 h. Cells were subjected to a robust analysis using FACStarPLUS with a laser excitation of 200 mW. DBA and cytokeratin were obtained from Vector Laboratories (Burlingame, CA) and Sigma Aldrich (St. Louis, MO), respectively.

Calcium Measurements

Differentiated cells were loaded with Fura-2AM (Molecular Probes, Eugene, OR) and placed in a perfusion chamber of 0.0254 cm thick and 1 cm wide. A shear stress of 0.78 dyne/cm² was applied to mouse epithelial cells. A range of shear stress from 0.1 to 5.0 dyne/cm² was

applied to determine the optimal fluid-flow stress for the human cells. All cells were subjected to fluid flow for at least 90 s. An interval of 30 min was used to rechallenge the cells with a second and third fluid-shear stress. Paired Fura-2 images were captured every 5 s at excitation wavelengths of 340 and 380 nm. The changes in signal intensity were captured in the horizontal plane close to the middle of the cells, and the objective was focused on the fluorescence signal of Fura-2. The basal levels of calcium were not significantly different between groups (Table 1).

Immunofluorescence

Cells were fixed with 2% sucrose plus 3% paraformaldehyde; permeabilized with 0.5% (vol/vol) Triton-X; and incubated with rabbit anti-polycystin antibody pMR3 (14) to detect human PC1, p96521 (10) to detect mouse PC1, or p96525 (15) to detect PC2. Antibodies were used at 1:200 dilution. For staining in RCTE and 9-12 cells, pMR3 was diluted to 1:1000 and applied to the cells for overnight incubation at 4°C to decrease nonspecific binding. Mouse antibody to acetylated α -tubulin (1:10,000; Sigma Aldrich) was used as a ciliary marker, and cells were counterstained with 4',6-diamidino-2-phenylindole (DAPI; Vector Laboratories) to label the nuclei. Differential interference contrast images also were acquired at this time. Adobe Photoshop 6.0 (Adobe Systems, Mountain View, CA) and NIH ImageJ 1.30 (Bethesda, MD) were used to reconstruct confocal images. Respective secondary antibodies were used at a dilution of 1:500.

Immunoblotting

The co-immunoprecipitation study was carried out according to the protocol from Upstate Biotechnology (Lake Placid, NY) to study the presence of and interaction between PC1 and PC2. Antibodies to polycystin at a dilution of 1:100 were used to pull down polycystin (PC1 or PC2). The primary antibody to the polycystins was blotted at a dilution of 1:1000 followed by a secondary anti-rabbit IgG antibody (1:5000). In cases that required signal amplification, biotinylated rabbit-specific antibody was used followed by the addition of streptavidin-conjugated horseradish peroxidase. For immunoblotting studies, pMR3 (14) and 7e12 (16) were used to detect human PC1, whereas p96521 (10) was used for mouse PC1. We used p96525 to detect either mouse or human PC2 (15). The high-molecular-weight protein marker was obtained from Amersham Biosciences (Piscataway, NJ).

Mutational Analysis

The complete *PKD1* and *PKD2* genes were screened in 9-12 and 9-7 cells by denaturing HPLC as described previously (17). Fragments that showed variant profiles were sequenced directly to characterize the mutation. Both a restriction digest using the enzyme *Hpy*CH4V and

Table 1. Baseline calcium and flow-induced calcium peak^a

	Mouse			Human				
	<i>Pkd1</i> ^{+/+} (n = 6)	<i>Pkd1</i> ^{+/null} (n = 6)	<i>Pkd1</i> ^{null/null} (n = 8)	RCTE (n = 6)	9-12 (n = 6)	NK (n = 8)	NT (n = 7)	CysT (n = 12)
Baseline calcium (nM)	132 \pm 11	137 \pm 14	142 \pm 8	119 \pm 7	124 \pm 10	104 \pm 5	106 \pm 8	110 \pm 5
Calcium peak (nM)	377 \pm 36	399 \pm 50	149 \pm 8	350 \pm 64	128 \pm 8	268 \pm 62	266 \pm 47	115 \pm 5

^aADPKD, autosomal dominant polycystic kidney disease; CysT, cystic tubules from ADPKD kidneys; NK, normal kidney; NT, normal-looking tubules of ADPKD kidneys; RCTE, renal cortical tubular epithelia; 9-12, ADPKD cyst-lining epithelia. n denotes the number of monolayers. Fifty cells from each monolayer were randomly chosen for analysis.

direct sequencing were used to assay the Q2556X mutation in 9-7 and 9-12 cells.

Data Analysis

The changes in cellular calcium were analyzed by taking a $\times 20$ or $\times 60$ phase-contrast image before the flow assay. This phase-contrast image then was divided into four equal quadrants; within each quadrant, we randomly outlined 12 individual cells, resulting in a total of approximately 50 cells. This was done for all analyses unless stated otherwise. The phase-contrast image, with the markings of individual cells, was merged with the calcium fluorescence image. The phase-contrast and fluorescence images were acquired at the same x and y dimensions. In some cases, the individual outlined cells from the first phase-contrast image then were merged to a second phase-contrast image (taken after flow stimulation) to confirm that the cells had not shifted during the course of an experiment. All values are reported as mean \pm SE. N indicates the number of independent experiments/monolayers for a given sample.

Radiometric images were acquired with a Nikon Diaphot inverted microscope equipped with a Nikon Fluor objective (Avon, MA). Fura-2AM-loaded cells were alternately excited at 340 and 380 nm, and the images of the respective 510-nm emission were acquired with IPLab software. Cytosolic free Ca^{2+} concentrations were calculated with the formula $[\text{Cyt } \text{Ca}^{2+}] = \text{Kd} \times [(\text{R} - \text{Rmin}) / (\text{Rmax} - \text{R})] \times (\text{Fmax}/\text{Fmin})$, where Kd denotes the apparent dissociation constant of the Fura-2 indicator (145 nM), R is a ratio of 510-nm emission intensity with excitation at 340 and 380 nm, and Rmax and Rmin are fluorescence intensity ratios for the calcium-bound and calcium-unbound Fura-2 with excitation at 340 and 380, respectively. We have determined the Rmax and Rmin values to be stable and independent of cell type. Fmax and Fmin are the fluorescence intensity values of Fura-2 with excitation at 380 nm under the same conditions. The Ca^{2+} level was radiometrically calculated. Rmin (0.30 ± 0.01) and Rmax (6.00 ± 0.05) values denote the minimum and maximum radiometric signal ratios, respectively. The minimum fluorescence (Rmin) was obtained by incubating the cells in calcium-free solution that contained 2 mM EGTA and 10 μM ionomycin at pH 8.6 to optimize the ionomycin effect (18). After the minimum signal ratio was determined, the cells were incubated with excess calcium (10 mM) to obtain the maximum signal ratio (Rmax). Signal intensities were collected from individual cells, as well as from the whole cell population/monolayer. All the fluorescence measurements were corrected for autofluorescence (19).

Results

Given the role of PC1 in the transduction of shear stress at the cilium, we investigated the differences in mechanosensing ability of heterozygous *Pkd1^{+/null}* as compared with wild-type and homozygous *Pkd1^{null/null}* mouse kidney epithelial cells. Cellular genotypes were determined as described previously (12). When a shear stress of 0.75 dyne/cm², the set point for mouse kidney cells to respond to fluid flow, was applied to the apical surface of these cells, wild-type but not *Pkd1^{null/null}* cells responded to fluid shear, as described previously (10). It is interesting that *Pkd1^{+/null}* and wild-type cells increased cytosolic calcium to a similar degree (Figure 1a). No apparent changes in cytosolic calcium in the homozygous cells were observed within the shear-stress range of 0.1 to 5.0 dyne/cm². When changes in cytosolic calcium concentration from a sample of individual cells were analyzed, variations in the magnitude of the responses were seen within a cell population (Figure 1b).

Whereas *Pkd1^{null/null}* cells showed no change in cytosolic calcium concentration, both wild-type and *Pkd1^{+/null}* cells demonstrated calcium spikes when challenged with repeated fluid-shear stress (Figure 1c). As expected, ciliary PC1 expression was not seen in homozygous cells but was present in both wild-type and heterozygous cells (Figure 1d). These data demonstrate that there is no detectable difference in mechanosensing functions and ciliary polycystin expression/localization between wild-type and *Pkd1^{+/null}* cells, suggesting that *Pkd1* mutations are recessive at a molecular level with regard to the mechanical fluid-shear sensing and cystic kidney phenotype.

We next analyzed the mechanosensory function of human kidney epithelial cells to verify the loss-of-function hypothesis for cystogenesis in ADPKD, as well as the functional consequences of acquiring a second hit, if a somatic mutation is found. Immortalized human RCTE and cyst-lining epithelial (9-12) cells were compared for the presence of cilia and their response to fluid shear. To make a valid comparison between these two cell lines, we used cellular markers to verify their tubular origins. The generation and partial characterization of these immortalized cells have been reported previously (13). In our study, these cells were cloned further, and their expression of both epithelial and collecting tubule markers was verified by the presence of cytokeratin (20) and DBA (13,21), respectively (Figure 2a). The presence of primary cilia on the apical cell surface of these cells was confirmed by scanning electron microscopy (SEM, data not shown) and confocal microscopy (Figure 2b).

In mouse renal epithelia, the set point for inducing a calcium response to ciliary activation by shear stress is 0.7 to 0.8 dyne/cm² (10). However, this degree of shear stress was insufficient to trigger a calcium response in our immortalized human RCTE cell lines. Further studies with shear stresses of 0.1 to 5.0 dyne/cm² revealed that the set point for a shear stress that is necessary to stimulate homogeneous calcium signaling is larger for the normal human kidney epithelial cells (1.2 dyne/cm²) than for mouse cells (0.8 dyne/cm²). When human RCTE cell lines were challenged with a fluid-shear stress in the range of 1.2 dyne/cm², they responded by increasing the cytosolic calcium concentrations in a manner similar to that in mouse cells (Figure 3a). In contrast, when the 9-12 immortalized cyst-lining cells were subjected to the same shear stresses of 0.1 to 5.0 dyne/cm², they failed to respond with an increase in intracellular calcium concentrations. At optimal shear stress of 1.2 dyne/cm² (Figure 3b), flow-induced calcium spikes were clearly observed in RCTE cells (derived from normal kidney) but not in 9-7 cells (derived from cyst 7 of ADPKD patient 9) or in 9-12 cells (derived from cyst 12 of the same patient 9). When rechallenged, the 9-12 cells, unlike the RCTE cells, remained unresponsive (Figure 3c). Immunolabeling of 9-12 cells with an antibody specific to human PC1 (pMR3) (14) revealed the absence of PC1 staining in cilia, in contrast to that in the RCTE cell lines (Figure 4a). Thus, the ability of cells to increase intracellular calcium in response to fluid-shear stress correlates with the presence of PC1 in the primary cilium, which may reflect the high percentage (>85%) of ADPKD cases with a *PKD1* mutation. Because a minority of ADPKD cases have a mutation

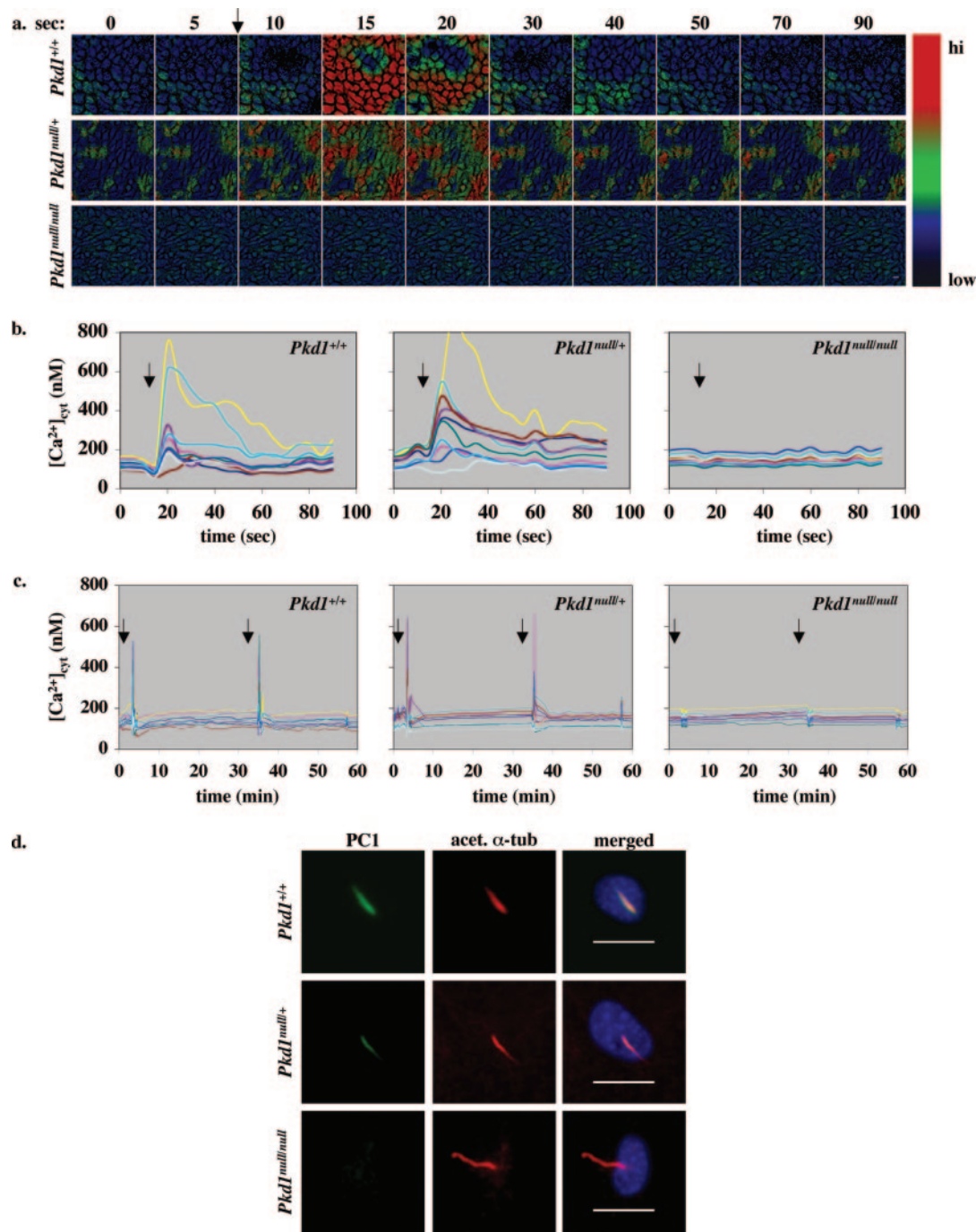


Figure 1. Heterozygosity of *Pkd1* mutation does not affect fluid flow sensing in mice. (a) The time-elapsed images of the responses of purified embryonic day 15.5 (E15.5) mouse collecting duct epithelia to a shear stress of 0.75 dyne/cm² are pseudocolored for cytosolic calcium level. The color bar indicates calcium level relative to baseline calcium level, with black and blue representing a low cytosolic calcium level (low) and green and red denoting a higher calcium level (hi). (b) Line graph of calcium response to flow sampled randomly from cells shown in panel a. A minimum of $n = 6$ for each genotype. (c) A repetitive response of representative calcium recording of 10 cells was shown for 1 h, when cells were rechallenged with 0.75 dyne/cm² fluid shear for a second time ($n = 4$ for each genotype). Fluid shear (arrow) was applied for 90 s after baseline calcium level was obtained. (d) When cells were stained with an antibody specific to mouse PC1 (p96521), failure to respond to shear stress corresponded to the disappearance of ciliary polycystin-1 in *Pkd1* homozygous cells. Polycystin-1 (PC1) counterstained with the nuclear marker 4',6-diamidino-2-phenylindole (DAPI) is co-localized with the ciliary marker acetylated α -tubulin (acet. α -tub). Bar = 10 μ m; original calcium images were taken with a $\times 20$ objective lens.

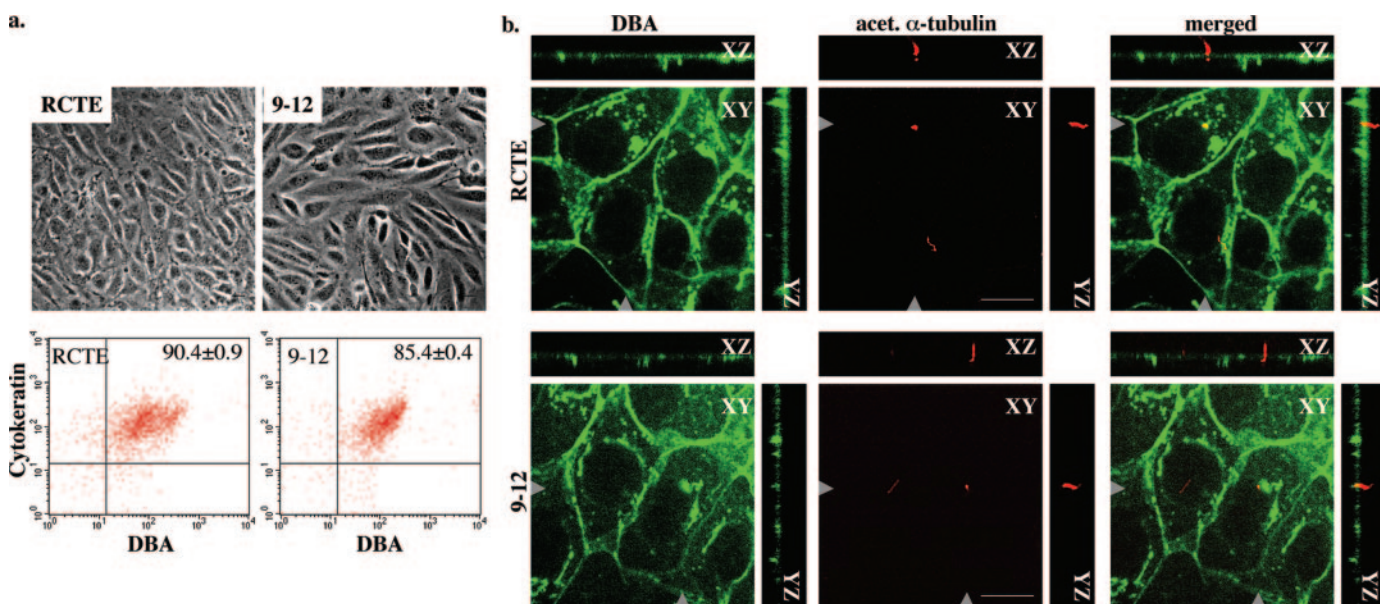


Figure 2. Immortalized human cell lines were characterized for morphology, expression of cell surface marker, and presence of cilia. (a) Normal (renal cortical tubular epithelia [RCTE]) and autosomal dominant polycystic kidney disease (ADPKD; 9-12) cell lines were compared morphologically after differentiation in serum-free medium for 3 d. The expression of epithelial (cytokeratin) and distal collecting (*Dolichus biflorus* agglutinin [DBA]) markers was confirmed in these cell lines by cell-sorting analyses. (b) The presence of cilia was analyzed by confocal microscopy in both RCTE and 9-12 cells. Cells were stained with the cilia-specific marker acetylated α -tubulin (red) and counterstained with the apical DBA marker in green. The XZ and YZ images were compiled from a stack of corresponding micrographs and projected at the cross-sections denoted by the gray arrowheads. Bar = 10 μ m; $n = 4$ for marker analysis and $n = 10$ for immunofluorescence in each cell line.

in *PKD2* (10 to 15%), we also examined PC2 expression in RCTE cells with an antibody to PC2 (p96525) (15). As expected, RCTE cells expressed PC2 on the primary cilium, but cilia of the 9-12 cells showed only faint or no staining, consistent with the role of PC1 as a regulator for normal expression, translocation, and function of PC2 (22–24). A trace level of PC2 localization in cilia in these PC1 mutant cells (Figure 4a) suggests that other factors also may modulate PC2 membrane targeting (15,25).

To verify the presence of PC2 in the RCTE cells, we co-immunoprecipitated lysates from both RCTE and 9-12 cells with PC2 antibody p96525 (Figure 4b-I, left). As expected, PC2 bands were seen in both lysates from the RCTE and 9-12 cells. It has been reported that PC1 and PC2 interact through the coiled-coil domains at their carboxyl-termini (22,26). To determine whether this interaction was preserved in the RCTE cells, we stripped and reblotted the same immunoprecipitation blot with the human PC1 antibody pMR3 (Figure 4b-I, right). The detection of PC1 in the PC2 immunoprecipitates in the RCTE cells supports the proposal of a cellular interaction between PC1 and PC2. Because the PC1 band was not seen in PC2 co-immunoprecipitates in 9-12 cells, we performed a reverse co-immunoprecipitation with PC1 (pMR3) antibody in both RCTE and 9-12 cells to determine whether the disruption of PC1–PC2 interaction was the result of the absence of PC1 protein in the 9-12 cell line. It is interesting that PC1 was detected in PC1 immunoprecipitates in RCTE but not in 9-12 cells (Figure 4b-II, left). When the same blot was stripped and

reblotted with PC2 p96525 antibody, the PC2 band was seen only in RCTE cells (Figure 4b-II, right). Thus, PC1 and PC2 co-immunoprecipitated in a reciprocal manner in the RCTE but not the 9-12 cells, indicating that the PC1 and PC2 interaction was maintained in the RCTE but disrupted in 9-12 cells.

To examine whether a truncated PC1 protein was present, we performed Western blot analysis on RCTE, 9-7, and 9-12 cells. Both 9-7 and 9-12 cell lines had truncated proteins, but the full-length PC1 was not observed in 9-12 cells (Figure 4c). Together, these data demonstrate the absence of full-length PC1 in the 9-12 cells, suggesting that both alleles of *PKD1* were mutated in this cell line. This was confirmed further by genetic analysis, which revealed a nucleotide substitution (7877C-T) that resulted in a truncation mutation, Q2556X, and an apparent homozygosity for this mutation in the 9-12 cells (Figure 4d), perhaps as a result of a somatic deletion of the normal allele in this region. In particular, the genetic data, along with the co-immunoprecipitation and Western blot data, explain why the 9-12 cells fail to respond to fluid flow shear stress.

The 9-7 cell line that was derived from another cyst of the same kidney also showed the Q2556X nonsense mutation (consistent with this being the germline change) but still retained the 7877C normal allele. Denaturing HPLC analysis of *PKD1* and *PKD2* in 9-7 cells revealed a new sequence change, A1302S, in *PKD1*. This sequence change has not been seen in *PKD1* in the normal human population; however, as it is serine in mouse and rat, it seems unlikely that this change is pathogenic. The chance of an unde-

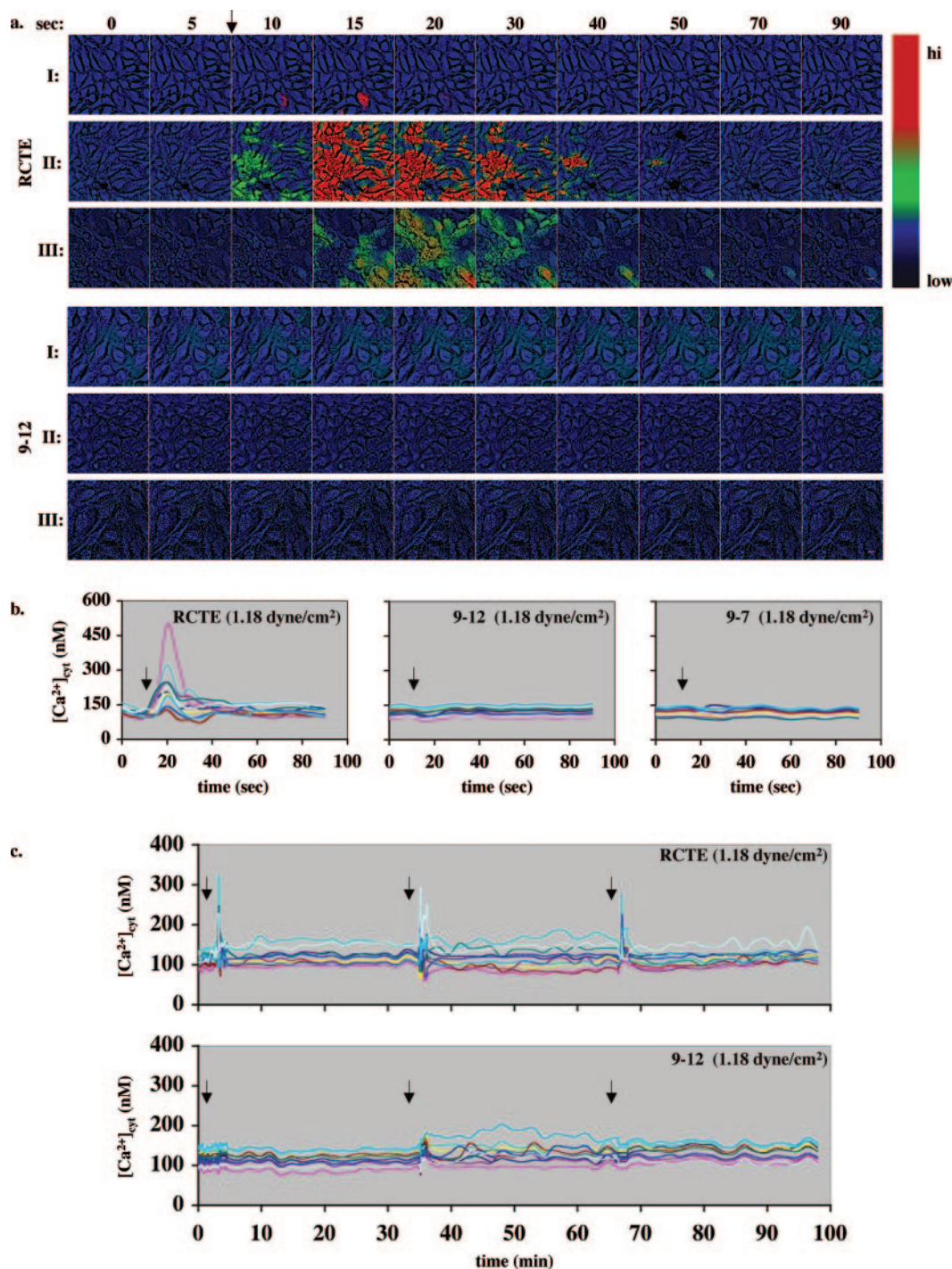


Figure 3. Cyst-lining cells derived from human ADPKD kidneys fail to respond to fluid-flow shear stress. (a) Fluid shear was applied after obtaining baseline calcium levels as indicated by arrow, and cytosolic calcium was recorded for 90 s. Both RCTE and 9-12 cells were challenged with different magnitudes of shear stress. The RCTE cells responded best to a shear stress of 1.18 dyne/cm² (II), less to 1.88 dyne/cm² (III), and not at all to 0.82 dyne/cm² (I). By contrast, the 9-12 cells did not respond to any of these shear stresses. The color bar indicates calcium level relative to baseline level, with black and blue representing a low cytosolic calcium level (low) and green and red denoting a higher calcium level (hi). For each genotype, $n = 6$ for 1.18 dyne/cm², $n = 3$ for both 0.82 and 1.88 dyne/cm², and $n = 1$ or 2 for other shear stresses (data not shown). (b) Line graph of calcium response to optimal shear stress of 1.18 dyne/cm² sampled randomly from 10 cells. Cytosolic calcium was recorded for 90 s; $n = 6$ for both RCTE and 9-12 cells; $n = 2$ for 9-7 cells. (c) Cytosolic calcium was recorded for >1.5 h. Images were captured at every 5 s. After the 90-s fluid-flow stimulation, the fluid flow was shut off for 30 min and cytosolic calcium was recorded continuously. A representative calcium recording of 10 cells is shown. All cells were rechallenged with 1.18 dyne/cm² fluid shear for a second and a third time as indicated by arrows; $n = 2$ for each genotype. Bar = 5 μ m; taken with a $\times 20$ objective lens. Arrows denote the onset of fluid shear stress.

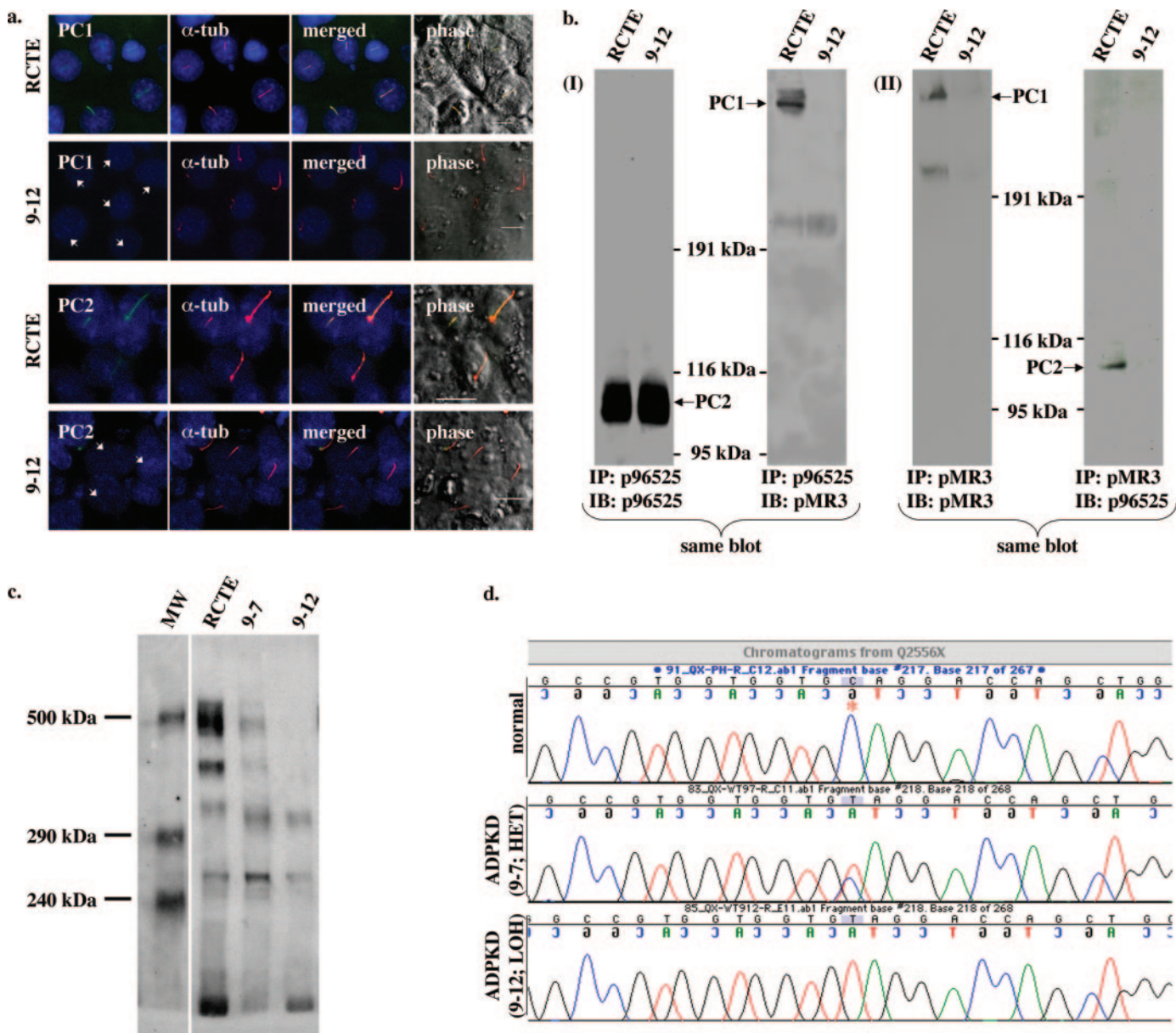


Figure 4. Cyst-lining cells derived from human ADPKD kidney are characterized by a mutation in PC1. (a) Both PC1 and PC2 are expressed in the cilia of the RCTE but not the 9-12 cells. Note that PC2 is localized to one of four primary cilia in 9-12 cells. Antibodies to human PC1 (pMR3, green) or PC2 (p96525, green) were used for co-localization with an antibody to a ciliary marker, acetylated α -tubulin (α -tub; red). Counterstaining with a nuclear marker (DAPI) is shown in blue, and differential interference contrast images are presented; $n = 5$ for each genotype. (b) Co-immunoprecipitation demonstrates that interactions between PC1 and PC2 are preserved in RCTE cells but not in 9-12 cells. PC1 expression is absent in 9-12 cells; $n = 1$ for b(I) and $n = 2$ for b(II). (c) Western blot analysis of PC1 is shown for RCTE, 9-7, and 9-12 cells. The 9-7 and 9-12 cells originated from nondilated (normal looking) and dilated (cystic) tubules of the same human kidney; $n = 1$. (d) Mutational analysis reveals that 9-12 cells (bottom) have an apparent homozygous mutation in *PKD1*, Q2556X. This may represent a hemizygous mutation and somatic deletion of the normal allele. Examples of the sequence from a normal (top) and the 9-7 cell line heterozygous for Q2556X (middle) also are shown. * denotes position of the nucleotide substitution; $n = 2$. Bar = 5 μ m.

tected somatic mutation in 9-7 cells remains, as the detection rate for denaturing HPLC in ADPKD is only approximately 65 to 70%. Unlike in mouse *Pkd1* heterozygous cells, 9-7 cells were unable to respond to fluid-shear stress with a typical calcium response (Figure 3b), consistent with the likelihood that these cells harbor an undetected somatic *PKD1* mutation. It is worth noting that these

human cell lines contain an SV40 large T-antigen gene that may affect their physiologic properties.

To verify the findings that were obtained from the immortalized mouse and human cell lines, we generated primary cell cultures to study the roles of the polycystins in epithelia that were derived from normal human kidneys and nondilated tubules and cysts

from kidneys of patients with ADPKD. Because of the limited supply of these cells, we chose to use a predetermined set-point shear-stress value of 1.2 dyne/cm² for the RCTE cells. We used only primary cultures with a morphologically homogeneous population for flow assay. Tubular epithelia were isolated from at least 24 different tubules of a normal kidney. Five of eight primary cultures displayed calcium signaling in response to a shear stress of 1.2 dyne/cm², and five of seven primary cultures that were derived from nondilated tubules of three ADPKD kidneys responded to the same shear stress. None of the 12 primary cell populations that were obtained from cyst-lining epithelia of three ADPKD kidneys showed a response to fluid-shear stress (Figure 5a). The relations between time and flow-induced cytosolic calcium changes were plotted for normal and ADPKD kidneys (Figure 5b).

Immunoblot studies of primary cell cultures were not feasible because of the limited number of cells, their short viability, and low expression levels of endogenous polycystins. Therefore, after the fluid flow-shear stress experiments, cells were fixed for immunofluorescence studies to examine the localization and expression of the polycystins (Figure 5c). All cells that responded to fluid-shear stress displayed normal expression and localization of PC1 and PC2 to the primary cilium. Analysis of 11 out of 12 cyst-derived cultures demonstrated mislocalization and/or abnormal expression of either PC1 or PC2, and in one case, we could not detect acetylated α -tubulin, a cilia marker, in cells 5 d after reaching confluence. In most cases, no ciliary PC1 or PC2 was detected

in cells that were derived from cystic/dilated ADPKD kidney tubules (Figure 5c, bottom). There also was no apparent difference in cilium length (8 to 12 μ m) among cell lines.

Discussion

Our study provides the first functional data supporting the molecular mechanism of the “two-hit” hypothesis and the loss-of-function model as an explanation for the pathogenesis of ADPKD. We also demonstrate for the first time that the polycystins are targeted to the primary cilia in primary and immortalized human kidney epithelial cells. Cysts start to develop at embryonic day 15.5 in *Pkd1* homozygous knockout mice (11,12); therefore, data from the E15.5 mouse cells demonstrate that loss of shear stress sensing is an early event in cyst formation and likely contributes to cystogenesis. To ensure that the mouse epithelial cells maintained their *in vivo* characteristics, we used cells with fewer than 20 passages and with the inactivation of the large T-antigen gene for at least 3 d before the experiment. Notably, *Pkd1* heterozygous cells, unlike the homozygous cells, still were able to respond to fluid shear, indicating that a germline mutation in an ADPKD gene is not sufficient to cause aberrant flow sensing, consistent with the absence of cystic phenotype in heterozygous mouse and human kidney at early ages.

We next determined whether we could use a fluid-flow assay to analyze the mechanosensory function of human kidney epithelial cells and thereby test the two-hit hypothesis of cystogenesis in

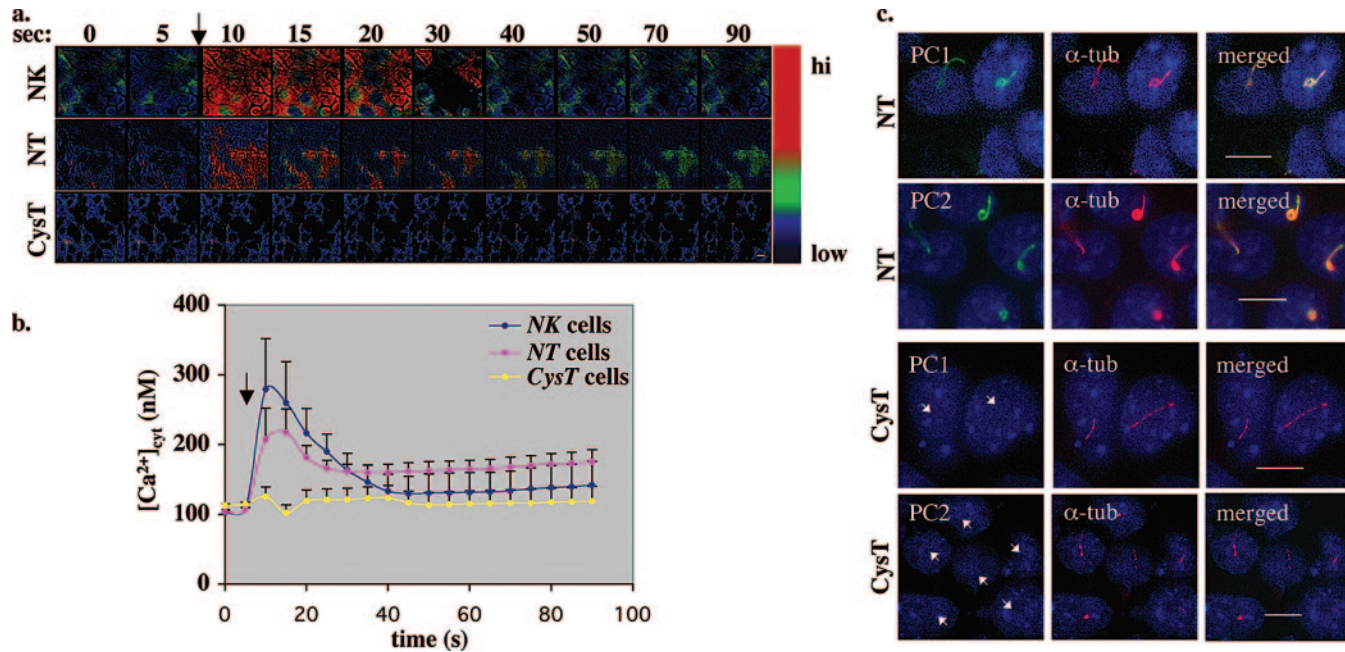


Figure 5. Failure of response to fluid-flow shear stress is associated with tubular dilation. (a) Human epithelial cells derived from normal kidney tubules (NK) and nondilated tubules (NT) of ADPKD kidneys respond to fluid-shear stress. Cyst-lining tubular epithelia (CysT) of ADPKD kidneys did not show any response to fluid-shear stress. Fluid shear was applied after the baseline calcium level was obtained as indicated by arrow. The color bar indicates calcium level relative to baseline calcium level, with black and blue representing a low cytosolic calcium level (low) and green and red denoting a higher calcium level (hi). (b) The average responses to shear stress were plotted in a line graph. (c) Expression of ciliary PC1 or PC2 is apparently absent in cyst-derived epithelia. Bar = 10 μ m; original calcium images were taken with a \times 60 objective lens. In all experiments, $n = 8$ for NK cells obtained from one noncystic kidney; $n = 7$ for NT cells obtained from three ADPKD kidneys; $n = 12$ for CysT cells obtained from three ADPKD kidneys.

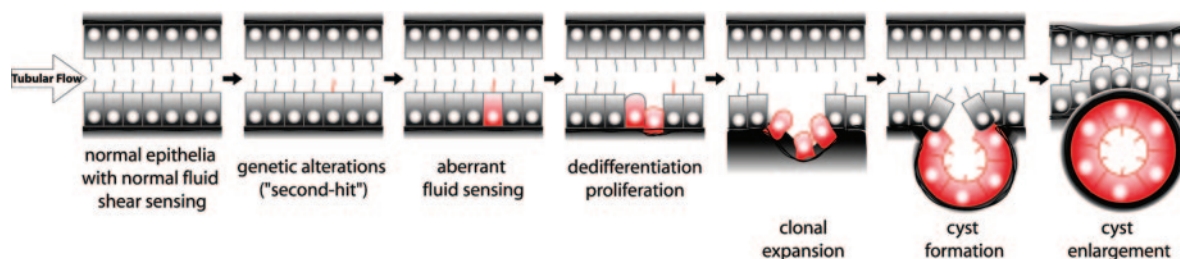


Figure 6. A hypothetical model illustrates the ciliary polycystins and cyst formation. Kidney epithelial cells from ADPKD patients are heterozygous for a germline mutation and retain their response to luminal fluid flow. Cyst-lining kidney epithelial cells lose their ability to sense mechanical fluid flow, probably as a result of the loss of the normal allele or the insult from genetic modification/variation. This may result in dedifferentiation and hyperproliferation of mutant cells, resulting in abnormal growth and unrestricted tubular lumen. The enlargement of the cyst may be facilitated by abnormal fluid transport into the lumen of the immature hyperproliferative cyst. The formation and enlargement of multiple cysts will eventually destroy surrounding functional nephrons, which may lead to end-stage renal failure.

human ADPKD, as well as the functional consequences of acquisition of a second hit. Immortalized RCTE cells that were derived from normal human kidney were compared with 9–12 cells that were derived from cyst-lining epithelia of a human ADPKD kidney. In our study, cyst-lining epithelial cells were cloned, and their expression of both epithelial and collecting tubule markers was verified. The presence of mechanosensitive cilia on the apical surface of these cells also was confirmed by SEM and confocal microscopy. The loss of response to fluid flow in tubular epithelial cells seems to correlate with the presence of a somatic mutation, the loss of interactions between PC1 and PC2, or the loss of PC1 expression in cells with a heterozygous PC1 mutation, suggesting that loss of mechanosensation is central to cystogenesis in humans with ADPKD.

Although the basal calcium levels of the different groups were not significantly different (Table 1), the calcium response to fluid-flow shear stress is variable for individual cells within a given cell population, as seen in the wild-type cells (Figure 1b). Because these mouse and human immortalized cells have been cloned, the variability in response within a given cell population could not reflect the presence of multiple cell types. These differences in the magnitude of response may reflect variations in the sensitivity of individual cells to mechanical stress, which can relate to the shape or surface topography of each cell and the position of each cell in the monolayer (27), and deserve further investigation.

In this study, we noticed that the cells required 30 min to respond to a second shear stress (Figures 1c and 3c). Stimulations at 5, 10, and 15 min after the first stimulation were unable to induce a second calcium spike, suggesting that the cells have a 30-min refractory period. The significance of this refractory period is presently unknown. Protein trafficking, channel inactivation/desensitization, cytoskeletal modifications, and cleavage and recycling of PC1 (28) in response to shear stress and the calcium spike might play a role in this timing.

Our data also suggest that in human cells, the primary cilium acts as a mechanosensory organelle with a set point for responding to fluid flow greater than that for mouse cells (1.2 versus 0.8 dyne/cm²). This difference probably is due to the

greater lumen size and/or rate of urine flow in the adult human kidney than in the embryonic mouse kidney. Such conservation in two-dimensional culture also suggests that the set point is not dependent solely on the cell geometry. The collecting duct in the rat is thought to experience shear-stress values in a range of 0.2 to 20 dyne/cm², depending on the rates of urine production (29). Therefore, the greater shear-stress values observed for the human cells are still within the minimum range of possible shear-stress values in the collecting duct. Furthermore, it also has been shown that developmental stages would alter the mechanosensitivity of kidney epithelia (30). In particular, a higher expression level of polycystins in the developing early kidney than in the adult kidney has been reported (31,32). We propose that, despite the wide range of physiologically relevant flow rates, primary cilia selectively sense a narrow range of low shear stress. This selectivity may be necessary for the control of cell proliferation and differentiation of tubular epithelia and, in turn, the maintenance of normal tubular lumen size and architecture. Therefore, in disease states in which the ciliary signaling is substantially altered, restriction in the lumen size is lost, possibly as a result of the loss of control of cell proliferation (33) and the guidance of planer cell polarity.

The results of our studies suggest that a second hit in addition to a heterozygous germline mutation is a prerequisite for the abnormal fluid sensing that leads to cystogenesis in ADPKD (Figure 6). Each differentiated kidney epithelial cell possesses a single cilium that senses fluid flow by increasing the intracellular calcium concentration; this signal normally may serve to inhibit cell growth and direct tissue expansion. The tubular epithelial cells of normal kidneys and heterozygous ADPKD kidneys are able to sense urinary flow along the tubular lumen and maintain tubular geometry. A second somatic hit on the normal copy of the *PKD* gene would disrupt the machinery that senses fluid flow, thereby making the cell effectively unresponsive to these normal regulatory signals that maintain tissue homeostasis. Complete loss of this form of mechanosignaling therefore may lead to a constitutive stimulus for growth that increases the lumen diameter and, hence, cyst formation.

Acknowledgments

We thank P. Finnerty and A. Beck for technical assistance. This work is supported by grants from the National Institutes of Health (DK40703, DK51050, and DK53357) to J.Z., the PKD Foundation (90a2r) to S.M.N., and NASA (NN-A04CC96G) to D.E.I.; S.M.N. and R.J.K. are supported in part by the National Institute of Diabetes and Digestive and Kidney Diseases Brigham and Women's Hospital Institutional Training Grant (DK07527-19).

References

- Reeders ST: Multilocus polycystic disease. *Nat Genet* 1: 235–237, 1992
- Brasier JL, Henske EP: Loss of the polycystic kidney disease (PKD1) region of chromosome 16p13 in renal cyst cells supports a loss-of-function model for cyst pathogenesis. *J Clin Invest* 99: 194–199, 1997
- Koptides M, Constantinides R, Kyriakides G, Hadjigavriel M, Patsalis PC, Pierides A, Deltas CC: Loss of heterozygosity in polycystic kidney disease with a missense mutation in the repeated region of PKD1. *Hum Genet* 103: 709–717, 1998
- Koptides M, Hadjimichael C, Koupepidou P, Pierides A, Constantinou Deltas C: Germinal and somatic mutations in the PKD2 gene of renal cysts in autosomal dominant polycystic kidney disease. *Hum Mol Genet* 8: 509–513, 1999
- Martin GM, Ogburn CE, Colgin LM, Gown AM, Edland SD, Monnat RJ Jr: Somatic mutations are frequent and increase with age in human kidney epithelial cells. *Hum Mol Genet* 5: 215–221, 1996
- Qian F, Watnick TJ, Onuchic LF, Germino GG: The molecular basis of focal cyst formation in human autosomal dominant polycystic kidney disease type I. *Cell* 87: 979–987, 1996
- Wu G, D'Agati V, Cai Y, Markowitz G, Park JH, Reynolds DM, Maeda Y, Le TC, Hou H Jr, Kucherlapati R, Edelmann W, Somlo S: Somatic inactivation of Pkd2 results in polycystic kidney disease. *Cell* 93: 177–188, 1998
- Pei Y, Watnick T, He N, Wang K, Liang Y, Parfrey P, Germino G, St George-Hyslop P: Somatic PKD2 mutations in individual kidney and liver cysts support a “two-hit” model of cystogenesis in type 2 autosomal dominant polycystic kidney disease. *J Am Soc Nephrol* 10: 1524–1529, 1999
- Nauli SM, Zhou J: Polycystins and mechanosensation in renal and nodal cilia. *Bioessays* 26: 844–856, 2004
- Nauli SM, Alenghat FJ, Luo Y, Williams E, Vassilev P, Li X, Elia AE, Lu W, Brown EM, Quinn SJ, Ingber DE, Zhou J: Polycystins 1 and 2 mediate mechanosensation in the primary cilium of kidney cells. *Nat Genet* 33: 129–137, 2003
- Lu W, Peissel B, Babakhanlou H, Pavlova A, Geng L, Fan X, Larson C, Brent G, Zhou J: Perinatal lethality with kidney and pancreas defects in mice with a targeted Pkd1 mutation. *Nat Genet* 17: 179–181, 1997
- Lu W, Shen X, Pavlova A, Lakkis M, Ward CJ, Pritchard L, Harris PC, Genest DR, Perez-Atayde AR, Zhou J: Comparison of Pkd1-targeted mutants reveals that loss of polycystin-1 causes cystogenesis and bone defects. *Hum Mol Genet* 10: 2385–2386, 2001
- Loghman-Adham M, Nauli SM, Soto CE, Kariuki B, Zhou J: Immortalized epithelial cells from human autosomal dominant polycystic kidney cysts. *Am J Physiol Renal Physiol* 285: F397–F412, 2003
- Geng L, Segal Y, Peissel B, Deng N, Pei Y, Carone F, Rennke HG, Glucksmann-Kuis AM, Schneider MC, Ericsson M, Reeders ST, Zhou J: Identification and localization of polycystin, the PKD1 gene product. *J Clin Invest* 98: 2674–2682, 1996
- Luo Y, Vassilev PM, Li X, Kawanabe Y, Zhou J: Native polycystin 2 functions as a plasma membrane Ca²⁺-permeable cation channel in renal epithelia. *Mol Cell Biol* 23: 2600–2607, 2003
- Ong AC, Harris PC, Davies DR, Pritchard L, Rossetti S, Biddolph S, Vaux DJ, Migone N, Ward CJ: Polycystin-1 expression in PKD1, early-onset PKD1, and TSC2/PKD1 cystic tissue. *Kidney Int* 56: 1324–1333, 1999
- Rossetti S, Chauveau D, Walker D, Saggar-Malik A, Winearls CG, Torres VE, Harris PC: A complete mutation screen of the ADPKD genes by DHPLC. *Kidney Int* 61: 1588–1599, 2002
- Nauli SM, Zhang L, Pearce WJ: Maturation depresses cGMP-mediated decreases in [Ca²⁺]i and Ca²⁺ sensitivity in ovine cranial arteries. *Am J Physiol Heart Circ Physiol* 280: H1019–H1028, 2001
- Nauli SM, Williams JM, Akopov SE, Zhang L, Pearce WJ: Developmental changes in ryanodine- and IP3-sensitive Ca²⁺ pools in the ovine basilar artery. *Am J Physiol Cell Physiol* 281: C1785–C1796, 2001
- Porter RM, Lane EB: Phenotypes, genotypes and their contribution to understanding keratin function. *Trends Genet* 19: 278–285, 2003
- Holthofer H, Schulte BA, Spicer SS: Expression of binding sites for *Dolichos biflorus* agglutinin at the apical aspect of collecting duct cells in rat kidney. *Cell Tissue Res* 249: 481–485, 1987
- Hanaoka K, Qian F, Boletta A, Bhunia AK, Piontek K, Tsikas L, Sukhatme VP, Guggino WB, Germino GG: Coassembly of polycystin-1 and -2 produces unique cation-permeable currents. *Nature* 408: 990–994, 2000
- Delmas P, Nauli SM, Li X, Coste B, Osorio N, Crest M, Brown DA, Zhou J: Gating of the polycystin ion channel signaling complex in neurons and kidney cells. *FASEB J* 18: 740–742, 2004
- Xu GM, Gonzalez-Perrett S, Essafi M, Timpanaro GA, Montalbetti N, Arnaout MA, Cantiello HF: Polycystin-1 activates and stabilizes the polycystin-2 channel. *J Biol Chem* 278: 1457–1462, 2003
- Kottgen M, Benzing T, Simmen T, Tauber R, Buchholz B, Feliciangeli S, Huber TB, Schermer B, Kramer-Zucker A, Hopker K, Simmen KC, Tschucke CC, Sandford R, Kim E, Thomas G, Walz G: Trafficking of TRPP2 by PACS proteins represents a novel mechanism of ion channel regulation. *EMBO J* 24: 705–716, 2005
- Qian F, Germino FJ, Cai Y, Zhang X, Somlo S, Germino GG: PKD1 interacts with PKD2 through a probable coiled-coil domain. *Nat Genet* 16: 179–183, 1997
- Davies PF: Flow-mediated endothelial mechanotransduction. *Physiol Rev* 75: 519–560, 1995
- Chauvet V, Tian X, Husson H, Grimm DH, Wang T, Hiesberger T, Igarashi P, Bennett AM, Ibraghimov-Beskrovnaya O, Somlo S, Caplan MJ: Mechanical stimuli induce cleavage and nuclear translocation of the polycystin-1 C terminus. *J Clin Invest* 114: 1433–1443, 2004
- Cai Z, Xin J, Pollock DM, Pollock JS: Shear stress-mediated NO production in inner medullary collecting duct cells. *Am J Physiol Renal Physiol* 279: F270–F274, 2000
- Liu W, Murcia NS, Duan Y, Weinbaum S, Yoder BK, Schwiebert E, Satlin LM: Mechanoregulation of intracellular

- lar Ca²⁺ concentration is attenuated in collecting duct of monocilium-impaired orpk mice. *Am J Physiol Renal Physiol* 289: F978–F988, 2005
31. Van Adelsberg J, Chamberlain S, D'Agati V: Polycystin expression is temporally and spatially regulated during renal development. *Am J Physiol* 272: F602–F609, 1997
 32. Geng L, Segal Y, Pavlova A, Barros EJ, Lohning C, Lu W, Nigam SK, Frischauf AM, Reeders ST, Zhou J: Distribution and developmentally regulated expression of murine polycystin. *Am J Physiol* 272: F451–F459, 1997
 33. Li X, Luo Y, Starremans PG, McNamara CA, Pei Y, Zhou J: Polycystin-1 and polycystin-2 regulate the cell cycle through the helix-loop-helix inhibitor Id2. *Nat Cell Biol* 7: 1102–1112, 2005